

# DESIGN OF A 2.2 GEV ACCUMULATOR AND COMPRESSOR FOR A NEUTRINO FACTORY

R. Cappel, B. Autin, M. Chanel, J. Gareyte, R. Garoby, M. Giovannozzi, H. Haseroth, M. Martini, E. Métral, D. Möhl, K. Schindl, H. Schönauer, CERN, Geneva, Switzerland  
 I. Hofmann, GSI, Darmstadt, Germany  
 C. Prior, G. Rees, RAL, Chilton, Didcot, U. K.  
 S. Koscielniak, TRIUMF, Vancouver, Canada

## Abstract

The proton driver for a neutrino factory must provide megawatts of beam power at a few GeV, with nanosecond long bunches each containing more than  $1 \times 10^{12}$  protons. Such beam powers are within reach of a high-energy linac, but the required time structure cannot be provided without accumulation and compression. The option of a linac-based 2.2 GeV proton driver has been studied at CERN, taking into account the space charge and stability problems which make beam accumulation and bunch compression difficult at such a low-energy. A solution featuring two rings of approximately 1 km circumference has been worked out and is described in this paper. The subjects deserving further investigation are outlined.

## 1 THE H<sup>-</sup> BEAM DELIVERED TO THE PROTON DRIVERS

In the scenario presented in this paper, the beam delivered to the accumulator and compressor (see Table 1) is generated by the proposed H<sup>-</sup> Superconducting Proton Linac (SPL) [1] based on the use of the 352 MHz LEP cavities. The driver beam parameters are mainly dictated by the properties of the systems used to generate the pions (produced by the proton beam), and to collect and cool the muons (produced by the pion decay) to be used in neutrino generation.

For this, a new and promising scenario [2] is under study at CERN. It is proposed to use 40 and 80 MHz RF systems to capture, cool and phase-rotate pions and muons, downstream of the target. In contrast to induction linac scenarios [3], the number of proton bunches per pulse is not limited. This has deep implications on the design of the accumulator and compressor, as it opens up the possibility of increasing the number of bunches in the machine, thus reducing the intensity per bunch. There is a beneficial impact on many parameters in this scenario: the linac duty cycle, ring lattice, instability rise-times and bunch compression.

## 2 PROTON DRIVER RINGS

### 2.1 General Layout

The geometry of the proton driver rings is determined by the preference that has been given to install the two ma-

chines in the former ISR tunnel. This tunnel has 150 m mean radius, with a width of about 15 m and height of 4 m.

Table 1: Summary of linac output beam characteristics.

Parameter	Unit	Value
Mean beam power	MW	4
Kinetic energy	GeV	2.2
Rep. rate	Hz	75
Pulse duration	ms	2.2
# of micro-bunch trains $\times$ turns		$140 \times 660$
Pulse intensity		$1.5 \times 10^{14}$
Train spacing	ns	22.7
# of micro-bunches/train		5
Micro-bunch spacing	ns	2.84
Micro-bunch intensity		$3.3 \times 10^8$
Micro-bunch length	ns	0.5
Energy spread ( $2\sigma$ )	MeV	0.2
Energy jitter within pulse	MeV	$\pm 0.2$
Energy jitter between pulses	MeV	$\pm 2$
$\Delta p/p$ ( $2\sigma$ )		$0.08 \times 10^{-3}$
$\epsilon_l$	eVs	$0.2 \times 10^{-3}$
$\epsilon_{h/v}^* = \beta \gamma \sigma_{h,v}^2 / \beta_{h,v}$	$\mu\text{m}$	0.6

The choice of performing the bunch compression by means of a non-adiabatic process, imposes the use of two separate rings: one for accumulation of the linac micro-bunches and one for compressing the resulting macro-bunches. The RF cavities needed to perform the bunch rotation would be a potential source of problems if installed in the accumulator ring. Their high impedance and the unavoidably long filling time could drive beam instabilities during the accumulation period. The beam characteristics common to the two rings are given in Table 2.

The accumulator lattice has been designed at RAL. All the optics computations for the compressor have been carried out at CERN by using different codes [4, 5] including space charge effects.

### 2.2 Accumulator Ring

The accumulator ring is fed directly by the linac through a transfer line where beam collimation is also performed: 140 buckets out of 146 available are filled using an H<sup>-</sup> injection scheme over 660 turns. Five linac micro-bunches, chopped from eight, are injected into each bucket. The ring is equipped with a 44 MHz RF system of the type devel-

oped for LHC in the CERN-PS [6]. The RF voltage is increased during beam accumulation to compensate continuously the longitudinal space charge. Injection simulations predict four subsequent proton foil traversals, on average, after the initial  $H^-$  beam stripping, resulting in acceptable foil temperatures for the carbon stripping foil. The simulations also show that the fast synchrotron motion due to the large  $|\eta|$  helps obtaining smooth macro-bunches at the end of the process.

Table 2: Summary of output beam characteristics common to accumulator and compressor rings.

Parameter	Unit	Value
Pulse duration	$\mu s$	3.3
RF freq. $f_{RF}$	MHz	44.02
# of bunches/h		140/146
Bunch intensity	protons	$1.1 \times 10^{12}$
$\epsilon_l$	eVs	0.1
$\epsilon_{h/v}^* = \beta\gamma\sigma_{h,v}^2/\beta_{h,v}$	$\mu m$	50

The lattice of this machine, based on triplet cells, has been designed to optimise the  $H^-$  injection. In particular, the value of the dispersion function at the stripping foil has been adjusted to allow ease of painting. The values of the optical parameters for half a super-period are shown in Fig. 1, while the main lattice parameters are summarised in Table 3.

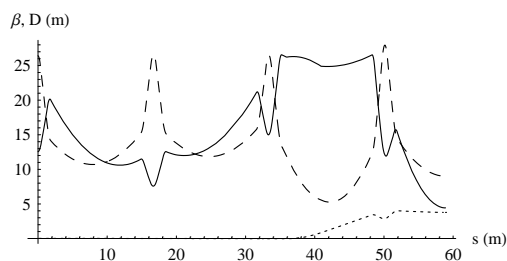


Figure 1: Optical parameters for the accumulator ring ( $\beta_h$  solid,  $\beta_v$  dashed,  $D_h$  dotted line).

Table 3: Summary of geometrical and optical parameters of the accumulator and compressor ring.

Parameter	Accumulator	Compressor
Radius (m)	151	151
Main dip. field (T)	0.69	0.49
$\gamma_{tr}$	14.837	15.089
$\eta$	-0.0848	-0.0849
$\beta_h^{\max}/\beta_v^{\max}$ (m)	26.4/26.2	24.5/25.5
$D_h^{\min}/D_h^{\max}$ (m)	0.0/4.6	0.0/1.8
$Q_h/Q_v$	11.23/13.30	17.18/16.40
Super-symmetry	8	8
Vac. pipe half width (m)	0.09	0.09
Vac. pipe half height (m)	0.09	0.09
# of dip.-quad./super-per.	3 – 22	5 – 17
Length of s.s./super-per. (m)	73.4	86.2

### 2.3 Compressor Ring

Once the accumulation process is over, the 140 macro-bunches are transferred to the compressor ring where their length is reduced by bunch rotation in less than  $30 \mu s$  (see Fig. 2). For that purpose the compressor ring is equipped with four cavities at 44 MHz [6], providing a total voltage of 2 MV, and with one cavity at 88 MHz [7] delivering 350 kV. Prior to beam transfer, RF power is applied to these cavities at a slightly offset frequency, so that the full voltages are present when the beam enters the machine. As soon as beam circulates, a peak beam current of about 15 A flows in the cavities. Since the bunch compression is much faster than the cavity filling time ( $100 \mu s$ ), the phase shift due to the transient beam loading increases almost linearly

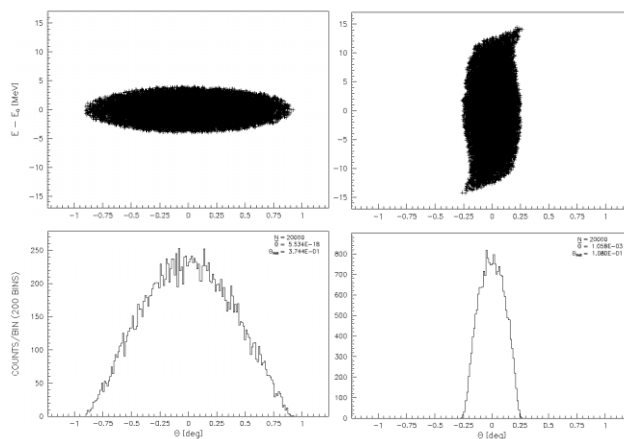


Figure 2: Bunch rotation in compressor ring. The phase portraits are shown in the upper part (initial left, final right). The projections along the direction of the azimuthal angle  $\theta$  are shown in the lower part (total horizontal scale  $\pm 1.23^\circ$ ,  $1^\circ = 9.21$  ns).

with time and can be compensated by an appropriate frequency difference between generator and beam frequencies ( $\approx 20$  kHz at 44 MHz). The compression process brings the bunches from the estimated initial r.m.s. length of 3.5 ns ( $\Delta p/p$  is  $1.5 \times 10^{-3}$  at  $2\sigma$ ) to the final one of 1 ns ( $\Delta p/p$  is  $5.0 \times 10^{-3}$  at  $2\sigma$ ).

The lattice of the compressor machine, based on doublet cells, has been designed to maximise the free space in the straight sections to allow the installation of the RF cavities. To this aim, the dispersion function is zero in the straight sections and special care has been taken to minimise the value of  $D_h^{\max}$  to reduce the transverse beam size of the rotated bunch. The values of the optical parameters for half a super-period are shown in Fig. 3, while the main lattice parameters are summarised in Table 3.

### 2.4 Space Charge and Other Collective Effects

Collective effects have been studied for both linac micro-bunches and macro-bunches at the end of the accumulation and compression processes. The transverse incoherent tune shift (for a particle at the centre of a transverse Gaussian,

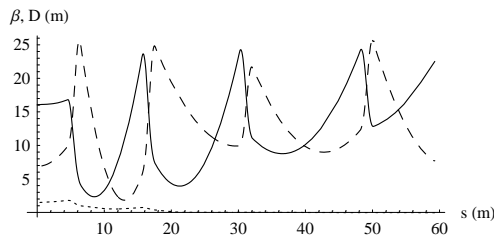


Figure 3: Optical parameters for the compressor ring ( $\beta_h$  solid,  $\beta_v$  dashed,  $D_h$  dotted line).

and longitudinally parabolic, bunch) of the macro-bunch at the end of the compression process is about  $-0.2$ , which is within the classical synchrotron limit. The RF voltage needed to match the macro-bunch at the end of the accumulation, including longitudinal space charge, is about 250 kV.

At the end of the accumulation, the Sacherer formula [9] for the macro-bunch interacting with the transverse resistive-wall impedance (using a resistivity of  $10^{-6} \Omega m$ ), yields rise-times of about 400 ms for the head-tail single-bunch instability, and 10 ms for the coupled-bunch instability. The growth-times are long compared to the 2.2 ms accumulation time.

The transverse mode-coupling instability [10] as well as the beam-breakup instability [11, 12] have also been investigated and are not harmful. The longitudinal coupled-bunch instability has been studied using the known Higher Order Modes (HOMs) of the CERN-PS 40 MHz RF cavity [8]. The computed rise-times [13] of the damped HOMs are much longer than the accumulation time. Finally, the longitudinal microwave instability has been studied using the coasting-beam formalism with the bunch peak current. In this computation, a broad-band impedance has been assumed at the cut-off frequency of the vacuum chamber ( $\approx 530$  MHz) with a unity quality factor. The plot of the rise-time vs. the broad-band impedance  $Z_{bb}/n$  is shown in Fig. 4. The accumulator ring should be carefully designed to have a broad-band impedance  $Z_{bb}/n \leq 1 \Omega$ . It

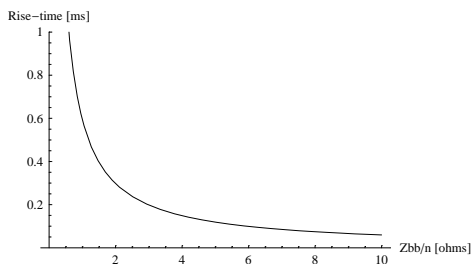


Figure 4: Microwave-instability rise-time (neglecting Landau damping) for the macro-bunch at the end of the accumulation process vs.  $Z_{bb}/n$ .

can be seen from Fig. 4 that in this case, the rise-time is about 0.6 ms, which is to be compared with the accumulation time (2.2 ms). Although the microwave instability could be a source of concern at first sight, preliminary simulation results show that it should not be a problem (tails of

the distribution provide Landau damping): the value of  $1 \Omega$  can be considered to be a conservative estimate.

### 3 CONCLUSIONS AND OUTLOOK

The study of a 2.2 GeV accumulator-compressor for a neutrino factory has shown that such an option is very promising, and no major obstacles have been found. The various parameters are not frozen, as their values depend on key components downstream of the proton drivers, such as targetry and cooling system.

Future activity will be devoted to refining the parameter list and to determining the optimal relative location of the two rings (whether they should lie on the same plane or should be separated vertically) with special emphasis on injection/extraction sections from the accumulator ring to the compressor ring.

More detailed investigations will be performed, by means of both analytical and numerical tools, to understand better the effects of the microwave instability and to investigate collective effects induced by electron clouds.

Finally, a campaign of numerical simulations will be carried out to study the issue of halo formation and beam losses in both rings.

### 4 REFERENCES

- [1] R. Garoby, M. Vretenar, "Status of the Proposal for a Superconducting Proton Linac at CERN", *CERN PS (RF)* **99-064** (1999).
- [2] A. Lombardi, "A 40-80 MHz System for Phase Rotation and Cooling", *CERN NuFact Note* **20** (2000).
- [3] R. Scrivens, "Example Beam Dynamic Designs for a Neutrino Capture and Phase Rotation Line Using 50 m, 100 m, 200 m Long Induction Linacs", *CERN NuFact Note* **14** (2000).
- [4] B. Autin, C. Carli, T. D'Amico, O. Gröbner, M. Martini, E. Wildner, *CERN* **98-06** (1998).
- [5] P. Bryant, WinAgile, private communication.
- [6] R. Garoby, D. Grier, E. Jensen, "The PS 40 MHz bunching cavity", *CERN PS (RF)* **97-39** (1997).
- [7] D. Grier, E. Jensen, R. Losito, K. Mitra, "The PS 80 MHz cavities", *CERN PS (RF)* **98-021** (1998).
- [8] E. Jensen, R. Hohbach, A. K. Mitra, R. L. Poirier, in *EPAC'96*, edited by J. Poole et al. (IOP, London, 1996) p. 2068-70.
- [9] F. J. Sacherer, in *Int. Conf. on High Energy Accelerators*, edited by US Atomic Energy Commission (CONF 740522, Washington D.C., 1974) p. 347-51.
- [10] R. D. Kohaupt, "Head Tail Turbulence and the Transverse PETRA Instability", *DESY* **80-22** (1980).
- [11] K. Yokoya, "Cumulative Beam Breakup in Large-Scale Linacs", *DESY* **86-084** (1986).
- [12] D. Brandt, J. Gareyte, in *EPAC'88*, edited by S. Tazzari (World Sci., Singapore, 1989) p. 690-92.
- [13] F. J. Sacherer, in *PAC'77*, edited by IEEE (Trans. Nucl. Sc., 24, 1977) p. 1393-95.